Guided-Ion-Beam and ab Initio Study of the Li^+, K^+, and Rb^+ Association Reactions with Gas-Phase Butanone and Cyclohexanone in Their Ground Electronic States†

J. M. Lucas,‡ J. de Andrés,‡ E. López,‡ M. Albertí,‡ J. M. Bofill,§ D. Bassi,|| D. Ascenzi,|| P. Tosi,|| and A. Aguilar*,‡

Departament de Química Física and Departament de Química Orgànica, Institut de Química Teòrica i Computacional (IQTCUB), Universitat de Barcelona, Martí i Franquès, 1, 08028 Barcelona, Spain, and Dipartimento di Fisica, Università degli Studi di Trento, 38050 Povo-Trento, Italy

Received: May 26, 2009; Revised Manuscript Received: July 21, 2009

The association reactions between Li^+, K^+, and Rb^+ (M) and butanone and cyclohexanone molecules under single collision conditions have been studied using a radiofrequency-guided ion-beam apparatus, characterizing the adducts by mass spectrometry. The excitation function for the $[M-(molecule)]^+$ adducts (in arbitrary units) has been obtained at low collision energies in the 0.10 eV up to a few eV range in the center of mass frame. The measured relative cross sections decrease when collision energy increases, showing the expected energy dependence for adduct formation. The energetics and structure of the different adducts have been calculated ab initio at the MP2(full) level, showing that the M^+-molecule interaction takes place through the carbonyl oxygen atom, as an example of a nontypical covalent chemical bond. The cross-section energy dependence and the role of radiative cooling rates allowing the stabilization of the collision complexes are also discussed.

Introduction

Since the pioneering work of Beauchamp et al.,[1] it is well-known that alkali ions, with particular reference to lithium and potassium, react with relatively simple molecules like halogenated organic and alcohols[2] and associate with many others, as proved by Hogg and Kebarle[3] who reported on the clustering of water molecules around K^+ in 1965. Moreover, alkali ion-alkali atom collisions have also received much attention since the first experimental studies done by Perel et al.,[4] Aquilanti et al.,[5] and Olsen et al.[6] considering symmetrical and unsymmetrical ion-atom pairs. The simple, one-electron, open-shell structure of the alkali ions allowed Aquilanti[7] and McMillan[8] to improve early model studies for these systems. More recently, other systems involving heavier alkali ions and atoms (in the few kiloelectronvolt energy range in the laboratory frame) have been studied[9] by some of us, using also Mg atoms as targets[10,11] complemented with multisurface dynamical studies for the $(Rb-Mg)^+$ system.[12] Nonadiabatic excitation charge transfers have been observed[13] in collisions between Li^+ and CdI_2, as well as collision-induced dissociations producing Cd atoms in excited electronic states. While the main interest of high-energy studies is their possible application in fields as ionized plasmas at low density,[14] lower collision energies have also attracted much attention as they play a role in many atmospherical[15] and biological systems.[16]

Light alkali ions, like sodium and potassium and, to a lesser extent, Li^+, interact with a variety of biologically important peptides and proteins, participating in, among other processes, enzyme regulation, the stabilization of structural elements, and transport through transmembrane channels to mention a few. In recent years, adduct formation between sodium ions and small biologically relevant molecules has been extensively studied by mass spectrometry, as comprehensively reviewed by Hoyau et al.[17] Such authors also performed new experimental studies using pulsed ionization, high-pressure mass spectrometry of sodium ion adducts with some small molecules and established a reliable absolute Na^+ affinity scale. Similar measurements had been previously carried out[18] to determine the binding enthalpies and entropies for many Na^+ adducts with small organic and inorganic molecules. Measured bond dissociation energies[17] for different adducts between Na^+ and small molecules were not much in agreement with previous data,[18] but collision-induced dissociation (CID) studies[19] supported Hoyau's results for different alcohols. Later, Armentrout and Rodgers[20] increased the experimental database measuring directly the absolute dissociation energies of different Na^+-molecule adducts using threshold CID in a guided ion beam-mass spectrometry experiment. The experimental studies were complemented by theoretical calculations at the Möller-Pleset second-order perturbation theory level (MP2),[21] and the combination of experimental and theoretical calculations provided a solid foundation for an absolute Na^+ affinity or bonding energy scale.

Ion-molecule association reactions and their application to mass spectrometry have been reviewed by Fujui.[22] This review is primarily concerned with thermal and three-body ion association reactions and includes reaction mechanisms, instrumentation techniques, and applications to mass spectrometry. Moreover, it provides reaction rates for several compounds and for ion-molecule association reactions, together with a comprehensive ion affinity tabulation, corresponding to standard enthalpy change (ΔH^o). While Li^+ is less effective than Na^+ and K^+ in biological systems,[16] it is remarkable for its prompt formation of solvated complexes and ion aggregates[23] and for the unique properties of Li^+ attachment in mass spectrometry applied to

† Part of the "Vincenzo Aquilanti Festschrift".

* Corresponding author. E-mail: a.aguilar@ub.edu.
‡ Departament de Química Física, Universitat de Barcelona.
§ Departament de Química Orgànica, Universitat de Barcelona.
|| Dipartimento di Fisica, Università degli Studi di Trento.

10.1021/jp904910d
Published on Web 08/19/2009

the detection of radical species in the gas phase.[22] Moreover, the formation of solvated complexes and ion aggregates are processes that affect chemical reactions, either directly or through its kinetic salt effect.[24] A detailed understanding of the noncovalent interactions between Li^+ and electron donor molecules forming solvated complexes can be found in studies[25] where a combination of matrix-assisted laser desorption ionization (MALDI) and Fourier transform ion cyclotron resonance (FT-ICR) techniques was used. In that paper, ab initio calculations of dissociation energies, geometries, and frequencies of the normal vibrational modes for the different lithium complexes were used to estimate which vibrational modes played a prominent role in the infrared (IR) emission leading to stabilization of the ion-molecule complexes formed under single collision conditions. FT-ICR techniques plus electron impact ionization of Na vapors were also used, in combination with ab initio studies, to unravel the nature of the binding in gaseous complexes of Na^+ with several molecules, including aromatics, by giving accurate enthalpies and entropies for complex formation reactions.[26]

More recently, Operti and Rabezzana[27] reviewed the determination of bond energies in gas phase organometallic systems, focusing on experimentally measured ion-molecule binding energies and on the experimental techniques used. The review included, in addition to the lighter ion-molecule adducts, information on Rb^+ and Cs^+ complexes, as well as on some alkaline earths and other metallic atoms. Considering the important role of serine and threonine in many biological systems, Armentrout and co-workers[28] measured their binding affinities with Li^+, Na^+, and K^+ by threshold collision induced dissociation (TCID) experiments showing that they are very similar to one another following the order $Li^+ > Na^+ > K^+$. Their experimental results were in agreement with different ab initio quantum chemical calculations.

Two years ago, we developed and built in our laboratory, in collaboration with the Atomic and Molecular Physics Group at Trento University (Italy), a radio frequency guided ion beam (RF-GIB) apparatus[29] that, in its present configuration, can be used to study ion-molecule systems in the energy range of few electronvolts or even a fraction, in the laboratory frame (LF). With this apparatus, we studied the acetone-Li^+adduct formation motivated not only from basic research interest[25] but also from an environmental issue[29] and previously studied by Woodin and Beauchamp[30] by ICR spectroscopy. For this system,[29] the cross-section (in arbitrary units) energy dependence was obtained. Using the newly developed RF-GIB apparatus, we have also studied[31] the dehydrohalogenation reaction of the *i*-C_3H_7Cl induced by collisions with Li^+ ions. Cross-section energy dependence for the two most important HCl elimination channels were measured in the center of mass (CM) 0.20−4.00 eV energy range (previously observed in crossed molecular beams by Creasy and Farrar[32]), as well as the excitation function for the chemical decomposition of the formed transitory $[Li-C_3H_7Cl]^+$ adduct leading to $C_3H_7^+$ formation. Following the research lines of the work carried out so far in our laboratory about systems of interest for organic chemistry and biochemistry, we present here a study on adduct formation of alkali Li^+, K^+, and Rb^+ ions with butanone (C_4H_8O) and cyclohexanone ($C_6H_{10}O$) molecules. For both ketones, the cross-section energy dependence for adduct $[M-(ketone)]^+$ formation has been measured in arbitrary units under single collision conditions at low CM energies. Moreover, to interpret the experiments even at a qualitative level, some knowledge of the interactions between partners is necessary. To get information about the structure and energetics of the adducts and the potential energy surface (PES) along which the association reaction takes place, complementary quantum chemical ab initio calculations have been carried out, exploring and investigating the main traits of the low-lying singlet potential surface adiabatically correlating the ion-molecule adduct with the ground electronic state reactants. The binding energies and geometries of all the experimentally studied adducts have been calculated, and an interpretation of adduct formation via stabilization of the collision complex by the radiative cooling process is presented.

Experimental Section

As the RF-GIB was previously described in detail,[29] here we will briefly outline its main features: a pure M^+ ion beam is generated by heating to about 1200 K a *spodumene* pellet, extracted by an adjustable potential, collimated, focalized, and collimated again prior to injection into an octopolar ion guide where ions are transversally trapped by a radio frequency (RF) field. The ion guide is shielded by a stainless steel sleeve which also defines the scattering cell volume. Neutral target gas is injected into the scattering cell at a pressure low enough to avoid multiple collisions. The octopole field is used both for primary beam guidance and for product gathering in a 4π steric angle. At its exit, all ions are collected by a second Einzel lens system and injected into a quadrupole mass analyzer. After mass selection, ions are finally detected by means of a Faraday cup. Background pressure is kept in the range of 10^{-6} mbar during experiments. The vapor pressures at room temperature of high purity butanone (MEK) and cyclohexanone (CHK) liquids are introduced in the scattering cell through a vacuum pipeline with individual purging. Vapor flows and pressures within the reaction cell (in the range of few 10^{-4} mbar)[29] are accurately controlled by a fine-pitch needle valve. A PC equipped with a suitable data acquisition interface controls the whole electronics with a software developed in our group using LABVIEW (National Instruments). Detailed information about the optimal working conditions for octopole ion guides, injection and extraction optics, ion mass analyzers, ion energy calibrations, and other relevant experimental details can be found in different references.[33−38]

The ion nominal LF kinetic energy is given by the difference between the extraction potential and the direct current voltage, or "bias", applied to the octopole rods. However, since the actual ion energy may differ from the nominal one, the so-called retarding potential analysis method[36] has been applied to measure the actual ion energy, using the octopole ion guide as a retarding energy analyzer. The obtained energy distribution is nearly Gaussian in shape,[29] with a typical full-width at half-maximum (fwhm) of about 0.7 eV measured in the LF frame. Consequently, for a nominal LF energy E_{lab}, the mean laboratory energy $\bar{E}_{lab}$ is given by

$$\bar{E}_{lab} = \int_0^\infty E \cdot P(E, E_{lab}) dE \qquad (1)$$

where $P(E, E_{lab})$ is the normalized distribution of the ion beam energy E which depends parametrically on the nominal energy E_{lab}. Assuming a stationary target molecule B of mass m_B and m_I being the ion mass, the CM relative kinetic energy E_0 is given by $E_0 = \bar{E}_{lab}(m_B)/(m_B + m_I)$, but the random motion of the target molecules inside the scattering cell leads to an

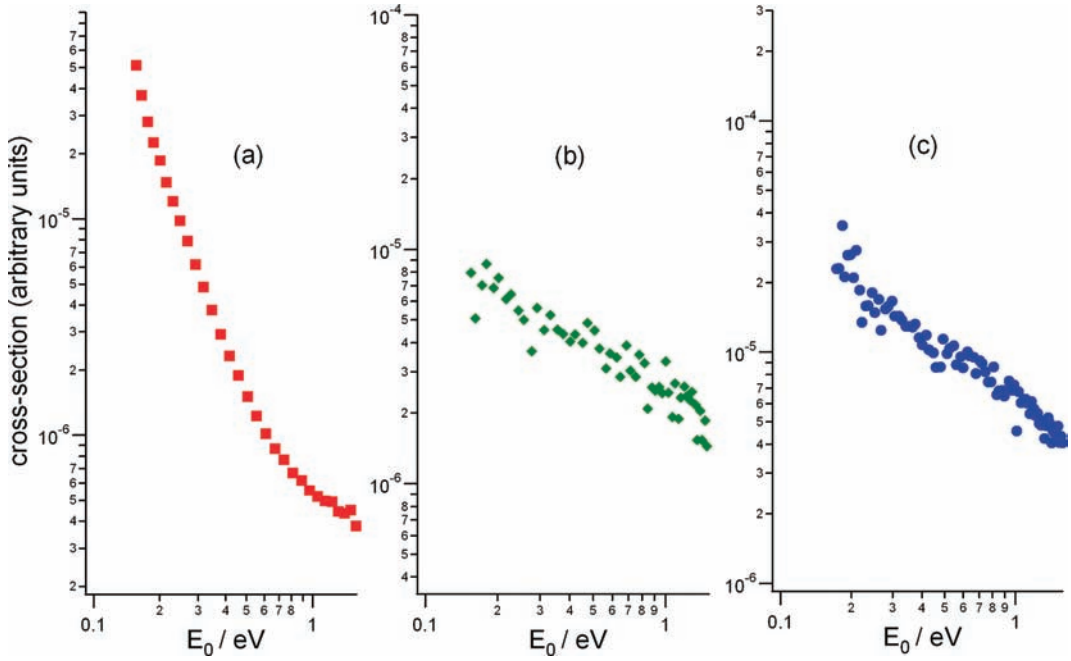

Figure 1. Measured cross-section energy $\sigma_{eff}(E_0)$ as a function of the CM relative energy (E_0) for butanone adducts: (a) $[Li-(C_4H_8O)]^+$, ■; (b) $[K-(C_4H_8O)]^+$, ♦; and (c) $[Rb-(C_4H_8O)]^+$, ●.

interaction energy distribution for each nominal energy of the incoming ion, showing the so-called Doppler broadening.[39−41] As a consequence, the measured cross-section as a function of the collision energy $\sigma_{eff}(E_0)$ may differ significantly from the true one $\sigma(E)$. Assuming a monoenergetic ion beam, both cross sections in the CM frame are related[36,37] by the convolution integral

$$\sigma_{eff}(E) = \int_0^\infty \left(\frac{E}{E_0}\right)^{1/2} f(E, E_0)\sigma(E)\mathrm{d}E \qquad (2)$$

where $f(E, E_0)$ is the Doppler interaction distribution. Consequently, our reported measured experimental data concerning association processes between ions and neutral MEK and CHK molecules refer to $\sigma_{eff}(E_0)$.

To obtain the σ_{eff}-energy dependence for the association reactions under study, $M^+(^1S_0)$ were extracted at 100.00 eV from the ion source, and the bias was varied between 102.00 and 90.00 V in 0.01 eV steps. The software-controlled quadrupole mass analyzer alternatively selects ions and adducts, and the corresponding signals are measured at each LF energy with an accumulation time of 0.1 s. For all adducts studied, the signal appears at relatively low energies and then quickly decreases until disappearing in the background noise. At a fixed value of the collision energy, it is possible to write

$$I_i/I_0 = \sigma_i n l \qquad (3)$$

where I_i and I_0 are the measured intensities (in arbitrary units) of the i-adduct and primary ions, respectively; σ_i is the energy-dependent cross-section for adduct formation; n is the i-target gas density in the scattering cell; and l is the effective path length. In our experiment, both n and l have not been measured, and therefore, only relative energy dependences of the cross sections are obtained.

Experimental Results

It is well-known that scattering processes between partners interacting through relatively strong potential wells (as those studied here) proceed by formation of long-lived complexes.[41] At the low collision energies explored in our experiments, the ion-molecule association reaction can be written as

$$M^+ + (\text{molecule}) \rightarrow [M-(\text{molecule})]^+ \qquad (4)$$

where M^+ is one of the ions (Li, K, Rb), and (molecule) refers to MEK or CHK. Under the usual experimental working conditions used throughout this paper, no signal for any possible adduct involving two or more target molecules was observed. $[M-(\text{molecule})]^+$ can stabilize via collisions with neutrals or photon emission, in competition with the back-dissociation to reactants.[25,27] At sufficient low target pressures, as those used in our experiments, IR photon emission is the main stabilization pathway. To ensure that $[M-(\text{molecule})]^+$ was not stabilized by secondary collision, some experiments were run at fixed ion beam energies, varying target pressure, and recording the corresponding adduct signal as a function of the estimated pressure inside the gas cell. The good linear dependence obtained in the range of 10^{-4} mbar according with eq 3 ensures that adduct formation takes place under single collision conditions as it also happened in the case of the $[Li-(C_3H_6O)]^+$ adducts.[29]

From the measured I_i and I_0 intensities, considering the primary ion beam energy spread and performing the LF to CM energy conversions, association cross sections ($\sigma_{eff}(E_0)$) as a function of the CM relative energy can be obtained. Figure 1 shows the cross-section (in arbitrary units) dependence from the collision energy in the CM frame for the adduct formed between MEK and all studied ions, while in Figure 2 the same magnitude is shown for the CHK adducts. In all cases, σ_{eff} shows a similar energy dependence, decreasing when the collision energy is increasing, as expected for thresholdless ion-molecule reactions controlled by long-range interaction potentials.

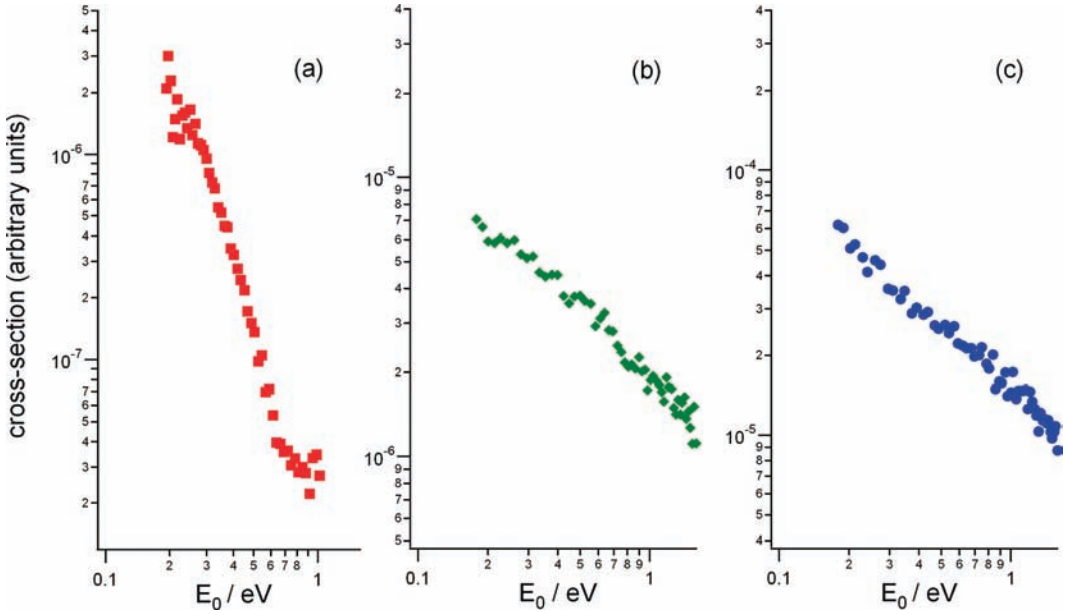

Figure 2. Measured cross-section energy $\sigma_{eff}(E_0)$ as a function of the CM relative energy (E_0) for cyclohexanone adducts: (a) $[Li-(C_6H_{10}O)]^+$, ■; (b) $[K-(C_6H_{10}O)]^+$, ♦; and (c) $[Rb-(C_6H_{10}O)]^+$, ●.

Ab Initio Structure Calculations. Any chemical reaction interpretation at the molecular level, even if only qualitative, requires information about molecular interactions on their evolution when reactants transform into products. In particular, the topological behavior of the potential energy surface (PES) at different points of the nuclear space coordinates (especially at possible reaction-relevant stationary points) must be known. As both reactants and ion-molecule adducts have a closed-shell electronic configuration in the entrance channel, we expect the reaction to proceed adiabatically on the ground singlet PES of the overall system. Electronic structure calculations for the ground singlet $[M-(molecule)]^+$ PES have been performed using the GAMESS 2006 computer program package.[43] For all adducts, calculations were carried out using the triple-ζ (TZV) basis set[44] that was estimated to represent accurately enough[31] the closed shell configuration of all participants. However, this basis set is not included in the package for Rb^+, so calculations involving this ion were performed using Pople's N-21G split valence basis set. Möller-Plesset second-order perturbation theory (MP2)[21] was applied using the molecular orbitals (MO) previously obtained in restricted Hartree-Fock (RHF)[45] calculations. To describe as well as possible the expected exoergicity of adduct formation, the core electrons were also taken into account in the calculation of the weak correlation energy (MP2(full)). In addition, the basis set superposition error (BSSE) has been taken into account using the algorithm implemented in the GAMESS program. According to this algorithm, the superposition error is considered mainly in the so-called strong electronic correlation effect.[46]

Starting from an ion-molecule separation of 15.000 Å and approaching both fragments, the calculated interaction energy does not show any potential energy barrier, and the supermolecule $M^+-(molecule)$ evolves to produce the $[M-(molecule)]^+$ adduct which is energetically below separate reactants. Energetics of the adduct formation process (ΔE) have been obtained performing ab initio calculations separately for each reactant, and the corresponding calculated values are given in Table 1. For both MEK and CHK reagents as well as for their adducts, a full geometry and energy optimization was done, and the zero point energy in the harmonic approximation (ZPE), routinely provided by GAMESS code, was calculated after a complete analysis of the Hessian matrix. Using the calculated electronic energies and ZPEs, reaction enthalpies (ΔH_0) or dissociation energies (D_0) at 0 K have been calculated, and their corresponding values are shown in Table 1. Concerning the figures for Rb^+ adducts reported in Table 1, their ΔE and D_0 values have been estimated by properly scaling the results of calculations for $[Rb-(molecule)]^+$ from values obtained for K^+ adducts in both TZV and N-21G basis sets. A close related procedure is described in ref 47. As can be seen in Table 1, calculated ΔE and D_0 values are quite similar, as expected if interactions between the alkali ion and the organic molecules do not involve covalent bonds, adduct formation being favored against reactants. Moreover, moving from Li^+ to Rb^+ and for both ketones, the calculated D_0 values decrease according with the corresponding ionic radii[48] increase and are in the same range as that calculated for the sodium−MEK adduct.[49] The BSSE corrections have minor effect over ΔE and D_0 calculated values, ranging from about 0.15 to 0.01 eV for Li^+ and K^+ complexes, respectively.

TABLE 1: Optimized Energies (ΔE) and Bond Dissociation Energies (D_0) for $[M-(Molecule)]^+$ Adducts at the MP2(full) Level Using the TZV Basis Set[a]

energetics/eV	$[Li-(molecule)]^+$	$[K-(molecule)]^+$	$[Rb-(molecule)]^{+b}$
(molecule) = C_4H_8O			
ΔE	−2.099	−1.024	−0.868
D_0	−2.038	−0.993	−0.842
(molecule) = $C_6H_{10}O$			
ΔE	−2.182	−1.077	−0.693
D_0	−2.119	−1.048	−0.671

[a] (molecule) = C_4H_8O, $C_6H_{10}O$; M = Li, K, and Rb. [b] Scaled values from the N-21 G basis set (see the text).

Although ion-molecule interactions leading to adduct formations are relatively strong (see D_0 values), they do distort the geometry of the original molecule only slightly. In Table 2 some of the most relevant atom-atom distances and bond angles are given. The original C−O distance increases about 0.01 Å when the adduct is formed, and the distortion diminishes on increasing alkali ion size. While it is difficult to compare results obtained

TABLE 2: Optimized Parameters for [M−(Molecule)]$^+$ Adducts (C_1 Symmetry) at the MP2(full) Level Using the TZV Basis Set, Where (Molecule) = C_4H_8O and $C_6H_{10}O$ and M = Li, K, and Rb

species	b.o.	C−O (Å)	M−O (Å)	∠M−O−C (deg)
C_4H_8O	1.932(1.783)[a]	1.261(1.235)[a]	-	-
$[Li-(C_4H_8O)]^+$	1.556	1.273	1.752	178.6
$[K-(C_4H_8O)]^+$	1.739	1.268	2.592	179.0
$[Rb-(C_4H_8O)]^{+a}$	1.660	1.259	2.759	176.2
$C_6H_{10}O$	1.965(1.779)[a]	1.262(1.252)[a]	-	-
$[Li-(C_6H_{10}O)]^+$	1.530	1.276	1.747	179.1
$[K-(C_6H_{10}O)]^+$	1.763	1.271	2.586	178.4
$[Rb-(C_6H_{10}O)]^{+a}$	1.639	1.260	2.748	178.3

[a] Results using the N-21 G basis set (see the text).

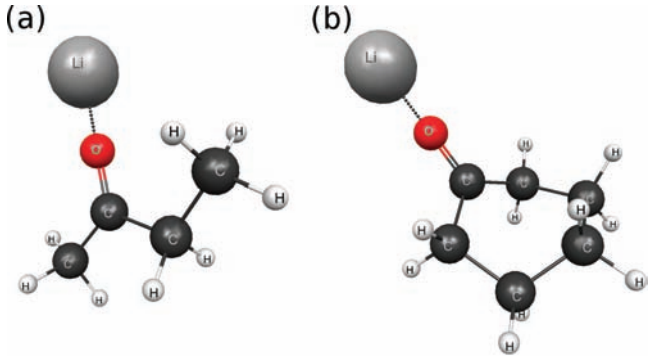

Figure 3. Optimized ground-state geometries of the $[Li-(C_4H_8O)]^+$ (a) and $[Li-(C_6H_{10}O)]^+$ (b) adducts. All structures were optimized at the MP2(full) level of theory.

using different basis sets, it can be appreciated that both K^+ and Rb^+ adducts show the lowest, very similar distortion (<0.01 Å). Moving from Li^+ to Rb^+, the O−M distance also increases (in agreement with the increasing ion size), and in the geometrically optimized adduct the alkali ion reaches a nearly collinear arrangement with respect to the C═O bond (see ∠M−O−C angle values in Table 2). The final geometries correspond to a C_1 symmetry for both the MEK and CHK adducts. Taking into account that the optimized geometries for the different adducts are very similar, and for the sake of brevity, only the most stable geometries of lithium adducts for both C_4H_8O and $C_6H_{10}O$ molecules are shown in Figure 3.

In addition to some of the optimized geometry parameters, Table 2 gives the bond order (b.o.) for the C═O bond in the species considered. From the table, calculated b.o. differences decrease in the sequence $Li^+ > K^+ > Rb^+$, tending to approach to the largest b.o. value of the isolated MEK and CHK molecules. From a chemical point of view, lower bond order values for $[M-(molecule)]^+$ adducts indicate a partial loss of the C═O double bond character, involving also an electronic charge density redistribution when moving from the asymptotic region of the PES to the potential well region describing the formation of the adduct. The increase in ion size from Li to Rb correlates with a decrease of the bond order of the carbonyl bond in the adduct, which results from the larger polarizing character of alkali ions according with the sequence $Li^+ > K^+ > Rb^+$. Adduct formation can be seen as a coordination process between alkali ions and ketone molecules, modifying the charge distribution both on the molecule skeleton and on the coordinated ion. An estimation of the charge distribution change can be obtained from a Mulliken analysis of atomic populations and charges on the adducts and on isolated reactants. This analysis for C_4H_8O adducts shows that only a small fraction of the electronic charge is transferred from butanone to the coordinating alkali ion, which keeps a net positive charge close to unity (Li: +0.909, K: +0.991). The largest changes are associated with the charge fraction on atoms involved in the carbonyl bond (isolated C_4H_8O: +0.256(C), −0.278(O); $[Li-(C_4H_8O)]^+$ adduct: +0.432(C), −0.573(O); $[K-(C_4H_8O)]^+$ adduct: +0.352(C), −0.487(O)). Roughly considered, atomic electronic charges on the carbonyl group increase about two times, the carbon atom becoming more positive and the oxygen atom more negative with regard to the isolated MEK. A similar behavior is found for $C_6H_{10}O$ adducts as proved by the following values of the electronic charge fraction: Li, + 0.903, K, + 0.991; isolated $C_6H_{10}O$, +0.230(C), −0.258(O); $[Li-(C_6H_{10}O)]^+$ adduct, +0.459(C), −0.577(O); $[K-(C_6H_{10}O)]^+$ adduct, +0.345(C), −0.482(O). In the case of the Rb adducts, the net charge of the cation decreases about 10% (as that for Li^+ shown before), while those on the carbon and oxygen increase much less, also when compared with previously mentioned adducts. The differences can be attributed to the lower quality of the basis set used in this case when compared to the TZV one.

From the MO analysis for the adducts optimized geometry, it follows that alkali atomic orbitals play a minor role describing occupied MOs (OMO) in the ion-molecule adduct but show large contributions in the description of the first virtual unoccupied MO (LUMO). The two highest (HOMO) largely describe atomic oxygen p-orbitals with a significant contribution of atomic carbon p-orbitals and a very small participation of the alkali atomic orbitals, explaining that, in the adduct, a large fraction of the positive charge remains on the original alkali ion.

Adduct formation adds three normal vibrational modes to those of the isolated molecule. Harmonic frequencies for both are shown in Table 3. Many of the adduct vibrational frequencies have values that are similar to the corresponding ones in isolated MEK or CHK, indicating a small perturbation on the original values as a consequence of adduct formation. Although any normal mode involves a displacement of all atoms from their equilibrium geometry configuration, in a first approximation, the three new normal modes can be classified as a stretching motion of the alkali ion-oxygen (M−O) bond and two bending motions involving angle (∠M−O−C) distortions, but the mixing of all atomic displacements makes it difficult to distinguish them clearly. However, for all adducts it is possible to identify a normal mode associated with the (M−O) bond. For MEK adducts, the corresponding vibrational frequencies occur at 564, 163, and 118 cm^{-1}, while for CHK ones they are 545, 161, and 112 cm^{-1} for M = Li, K, and Rb, respectively.

Moreover, the alkali adducts for each molecule show a vibrational frequency close to that assigned to the carbonyl stretching mode, i.e., 1616 cm^{-1} for C_4H_8O and 1598 cm^{-1} for $C_6H_{10}O$, respectively, in isolated molecules. The corresponding frequencies, for Li and K adducts, appear at 1635 and 1629 cm^{-1}, respectively, in the case of MEK and at 1616 and 1611 cm^{-1} for CHK. Thus, adduct formation shifts the original C═O vibration by less than 20 cm^{-1} for both C_4H_8O and $C_6H_{10}O$ adducts. When using the N21 G basis set, C═O stretching frequencies for the isolated MEK and CHK appear at 1667 and 1658 cm^{-1}, respectively, while they shift to 1685 and 1677 cm^{-1} in the corresponding rubidium adducts. Also in this case the shifting of the C═O vibration is below 20 cm^{-1}. These figures indicate that the vibrational mode associated with the carbonyl (C═O) bond of the isolated neutral molecule is only slightly perturbed by the presence of the alkali ion when the ion-molecule adduct is formed. However, the calculated increase

TABLE 3: Harmonic Vibrational Frequencies Optimized at the MP2(full) Level

species	frequencies (cm^{-1})
C_4H_8O	67, 158, 192, 259, 408, 486, 599, 771, 801, 981, 999, 1028, 1131, 1174, 1230, 1292, 1406,1458, 1480, 1510, 1522, 1527, 1539, 1547, 1616, 2969, 3003, 3005, 3015, 3077, 3086, 3105, 3129
$[Li-(C_4H_8O)]^+$	68, 94, 114, 150, 217, 264, 405, 488, 564, 598, 789, 818, 994, 1016,1040, 1138, 1184, 1258, 1296,1425, 1471, 1484, 1491, 1514, 1516, 1544, 1552,1635, 2986, 2992, 3013, 3023, 3077, 3096, 3118, 3127
$[K-(C_4H_8O)]^+$	45, 68, 98, 159, 163, 200, 274, 419, 492, 599, 784, 797, 993, 1004, 1035,1131, 1182, 1250, 1299, 1420, 1470, 1480, 1501, 1518, 1522, 1543, 1551,1629, 2977, 3011, 3013, 3027, 3088, 3095, 3103, 3127
$[Rb-(C_4H_8O)]^{+a}$	35, 68, 88, 118, 152, 217, 270, 416, 508, 589, 765, 807, 967,1027, 1029, 1136, 1197, 1222, 1355, 1411, 1473, 1498, 1549,1559, 1574,1599, 1604, 1685, 3078, 3088, 3097, 3120, 3156, 3169, 3184,3190
$C_6H_{10}O$	68, 120, 274, 390, 458, 491, 502, 624, 744, 791, 851, 893, 909, 938, 1008, 1058, 1107, 1120, 1157, 1167, 1248, 1282, 1292, 1309, 1360, 1369, 1396, 1415, 1416, 1496, 1502, 1525, 1538, 1541,1602, 2961, 2987, 2992, 2998, 3003, 3020, 3040, 3042, 3055, 3073
$[Li-(C_6H_{10}O)]^+$	49, 95, 119, 161, 272, 379, 447, 488, 506, 545, 663, 769, 794, 853, 882, 910, 933, 1007, 1051, 1102, 1125, 1161, 1176, 1248, 1284, 1301, 1314, 1347, 1371, 1402, 1418, 1419, 1478, 1493, 1525, 1541, 1542, 1615, 2965, 2988, 3001, 3013, 3017, 3039, 3047, 3066, 3079, 3086
$[K-(C_6H_{10}O)]^+$	37, 52, 106, 124, 161, 275, 397, 460, 490, 508, 631, 747, 791, 848, 888, 908, 934, 1006, 1054, 1103, 1123, 1160, 1172, 1248, 1283, 1296,1310, 1353, 1370, 1399, 1417, 1418, 1487, 1497, 1525, 1540, 1542, 1611, 2966, 2992, 2998, 3007, 3010, 3039, 3044, 3056, 3071, 3078
$[Rb-(C_6H_{10}O)]^{+a}$	34, 40, 91, 112, 145, 286, 398, 455, 473, 514, 632, 741, 793, 835, 891, 908, 939, 1001, 1047, 1075, 1133, 1163, 1194, 1277, 1287, 1324, 1339, 1370, 1387, 1420, 1424, 1427, 1538, 1558, 1582, 1594, 1597, 1677, 3071, 3081, 3097, 3102, 3111, 3127, 3131, 3148, 3162, 3167

[a] Results using the N-21 G basis set (see the text).

in vibrational frequency of the C═O stretching mode in the alkali ion adduct compared to the isolated molecule points out that (albeit quite weakly) the C═O bond strength has been increased. These results could be explained considering that the C═O sigma component becomes somewhat reinforced as a consequence of the low electronic charge transfer from the HOMO (mainly with the nonbonding oxygen orbitals of the carbonyl group) to the coordinated ion, previously discussed. In fact, moving from Li^+ to K^+, the transferred electronic charge decreases, thus decreasing the corresponding vibrational shifting in both the butanone clusters (Li: 19 cm^{-1}; K: 13 cm^{-1}) and the cyclohexanone ones (Li: 17 cm^{-1}; K: 13 cm^{-1}). In the case of the Rb^+ clusters, calculated vibrational shiftings are 18 and 19 cm^{-1} for MEK and CHK, respectively, and comparable with the previous ones.

Discussion

The ion−ketone association reactions reported here take place on a barrierless PES, so that they do not have any activation energy. Moreover, the relatively low interaction energy between partners forming the corresponding adduct leads only to minor changes in the structure of the original ketone molecule and in cation charge (which in all studied adducts behaves as a hard ion). Therefore, the binding can probably be primarily electrostatic.[48] MEK and CHK are dipolar molecules, and their electrostatic interaction with alkali ions can be seen as an overlap of different contributing interactions, mainly ion-permanent dipole, ion-induced dipole, and ion-quadrupole. In Table 2 and Figure 3, the ion in the adduct is always very well aligned with the dipole moment of the original molecule, as also observed in other sodium ion-organic molecule complexes.[17] The above-mentioned features confirm the essentially noncovalent nature of the bonding between alkali ions and MEK or CHK, with only minor changes of the ketone skeletal structure upon adduct formation.

It is well-known that barrierless reactions are usually controlled by the long-range part of the potential, which can also be very anisotropic. For these processes, the capture model approximation[50] has proved to give satisfactory results even between neutral radicals.[51]

Assuming that alkali ion-molecule associations are controlled by long-range interactions, at a given E_0 (CM), the total energy content of the collision complex is higher than the energy of the dissociation limit, leading to its decomposition into reactants. At very low pressures, where single collision conditions are achieved, the adduct stabilizes via photon emission, and in the absence of electronic excited states, infrared (IR) decays are chiefly responsible for a substantial reduction in the complex excess internal energy. The radiative rates for large molecules like these collision complexes can be calculated[52] as a function of their internal temperature T, which in turn is a function of their internal energy and heat capacity and depends on all the vibrational frequencies and their integrated absorption intensity. Considering that this energy is given by the binding plus the thermal ones brought into the complex by the two reactants, Dunbar[52] gives a broad estimation of the feasibility of radiative association as a function of the number of degrees of freedom (N) of the collision complex, classifying it as small (N of the order of 20), medium (N of the order of 60), and large size (N of the order of 200), as well as of the corresponding binding energy. For medium-sized complexes such as ours, an estimation of the binding energy gives a value of about 1.5 eV, and as can be seen from data in Table 2, calculated binding energies are qualitatively in agreement with the values estimated by Dunbar's empirical rule. These results show the important role of the rate of the IR radiative emission in stabilizing complexes formed under single collision conditions such as ours.

Taking into account the very important role played by long-range interactions between ions and molecules, and considering the capture model approach, different authors[53] give analytical cross-section energy dependences for such reactions. In general, all models can lead to a near linear energetic dependence of the cross-section with energy in a double logarithmic representation, so that σ behaves as a function of E^{-m}, where m is a fitting parameter. Furthermore, all models show as a general behavior a decrease of σ when energy increases, and as can be seen from Figures 1 and 2, our experimental dependences are qualitatively in agreement with such expectations. For a given polar molecule, the experimental results indicate that m depends on the alkali ion considered (approximate m-values for C_4H_8O adducts are: −2.5 (Li^+), −0.7 (K^+), and −0.6 (Rb^+), while for $C_6H_{10}O$ ones they are −3.5 (Li^+), −0.8 (K^+), and −0.8 (Rb^+)).

Figure 1 shows that $[Li-C_4H_8O]^+$ cross-section energy dependence presents a noteworthy curvature at the highest energies, diverging from the essentially linear dependence at low energies. Adducts with a common alkali ion have relatively close *m*-values. In spite of the $\sigma \alpha E^{-m}$ dependence found experimentally, estimated *m*-values can hardly be interpreted by the well-known models.[53] However, it is necessary to recognize that these models simplify very much the molecular structure, i.e., neglecting the internal degrees of freedom, which can play a particularly important role in association reactions such as these.

The measured cross sections from Li^+ to Rb^+ tend to increase roughly about 1 order of magnitude in the case of the MEK alkali ion adducts and about 2 orders of magnitude for CHK adducts. In a capture model and using the long-range interaction potential previously considered, the developed centrifugal barrier from an orbital angular momentum **L** (associated with the classical impact parameter **b**) plays a major role on the reactivity, centrifugal potential being given by $\mathbf{L}^2/2\mu R^2$ (where μ is the reduced mass of the two colliding particles and *R* the distance between the ion and the molecule center of mass). Taking into account that reaction cross-section equations[42,50] involve a summation over all possible values of the *L* quantum number associated with **L**, then a larger contribution of *L* values can be expected at a fixed collision energy when the reduced mass increases from lithium to rubidium, leading to an increase of the measured cross-section as experimentally found.

When the ion-molecule adduct is formed under single collision conditions, its internal energy is given by the binding energy plus the energy brought into the complex by the two colliding reactants. In the present experiments, target molecules are in thermal equilibrium at room temperature *T*, and their internal energies can be assumed statistical at the same temperature. Then, their average rotational energy is given by $3/2kT$, and their vibrational one can be calculated[54] using the molecule harmonic vibrational frequencies. Moreover, for a given E_0, a fraction of the translational energy is converted into internal energy of the collision complex. This moves as a single, nondissociating particle possessing the center of mass energy of the two colliding particles, given by $(m_I/m_B)E_0$ (where m_I and m_B are the ion and neutral molecule masses, respectively, and target molecules are stationary). Assuming that, upon adduct formation, the rotational energy is essentially conserved as such, an energy balance allows a straightforward calculation of the internal vibrational energy (which is in turn a function of E_0). The adduct internal temperature (T_{int}) can therefore be calculated assuming the statistical equation of the vibrational energy associated with a molecule with 3N-6 vibrational modes, the resulting T_{int} being also a function of E_0. According to Dunbar,[52] the frequency (υ_{max}) that most contributes to the radiative cooling rate of the collision complex is given[25] by $\upsilon_{max} = 2kT_{int}/h$, where *h* is Planck's constant.

In the collision energy range of interest in the present study, the υ_{max} values have been estimated at two different E_0 values, i.e., 0.10 and 1.00 eV. For $[M-(C_4H_8O)]^+$, calculated values of υ_{max} (in cm^{-1}) are: 1946 (0.10 eV, T_{int}= 1400 K), 2382 (1.00 eV, T_{int}= 1714 K) for Li; 1279 (0.10 eV, T_{int} = 920 K), 1540 (1.00 eV, T_{int} = 1108 K) for K; 1127 (0.10 eV, T_{int} = 811 K), 1006 (1.00 eV, T_{int} = 724 K) for Rb. For $[M-(C_6H_{10}O)]^+$, calculated values of υ_{max} (also in cm^{-1}) are: 1737 (0.10 eV, T_{int} = 1250 K), 2043 (1.00 eV, T_{int} = 1470 K) for Li; 1158 (0.10 eV, T_{int} = 833 K), 1425 (1.00 eV, T_{int} = 1025 K) for K; 920 (0.10 eV, T_{int}= 662 K), 991 (1.00 eV, T_{int} = 713 K) for Rb. Therefore, the IR frequency most contributing to the radiative cooling rate changes with collision energy, and taking into account that the radiative rate[52] is proportional to υ^2, the model predicts that higher internal energies will result in faster radiative cooling rates. Lighter adducts have the largest binding energy, but at the same time, they bring the largest E_0 fraction into internal energy. As a consequence, successful formation of a stable light adduct requires the highest IR frequency emission for an efficient cooling of the collision complex (see above). With increasing the ion mass, a smaller fraction of the collision energy is brought into the complex, and its radiative cooling becomes less critical but nevertheless is always necessary for the stabilization to take place.

Although the calculated υ_{max} values are E_0 dependent, the vibrational energy spectra of potassium and rubidium adducts show many vibrational frequencies relatively close to that value, while this is not the case for the lithium adduct, where vibrational frequencies are more separated. Thus, higher cross-section values can be expected for the potassium and rubidium adduct formation from both MEK and CHK molecules in agreement with our experimental findings.

Conclusions

The formation of adducts between alkali ions and butanone and cyclohexanone has been studied under single collision conditions using a RF-GIB apparatus. The corresponding σ (in arbitrary units) as a function of the collision energy has been measured between 0.10 eV and a few electronvolts depending on the system. Measured excitation functions decrease when the collision energy increases as can be expected for barrierless reactions controlled by long-range interaction potentials. Adduct formation is observed as result of a capture process by the alkali ion of a polar molecule on an adiabatic PES in competition with the unimolecular decomposition of the collision complex which can be stabilized by IR radiative emissions. The essential trends of the potential surface as well as the structure of alkali ion-molecule adducts have been studied by ab initio calculations at the MP2 level. Calculations show that the interaction between the alkali ion and the ketones is a noncovalent interaction between the nonbonding oxygen orbitals of the carbonyl group and the closed-shell ion, showing a small charge transfer that decreases from Li^+ to Rb^+ ions. Upon adduct formation, M^+ tends to be collinear with the ketone C═O bond, its skeleton being only slightly distorted by this process. Calculated binding energies decrease in the order $Li^+ > K^+ > Rb^+$ as a consequence of the decreasing interaction between reactants. Although given in arbitrary units, measured cross sections increase with the size of the hard closed-shell alkali ion showing a collision energy dependence qualitatively in agreement with those expected for reactions controlled by long-range interaction potentials. Moreover, the radiative cooling rate depends on the internal excitation energy of the collision complex formed in the bimolecular ion-molecule encounter. To the best of our knowledge, this is the first time that the cross-section energy dependence for the formation of the studied $[M-(molecule)]^+$ adducts has been reported under single collision conditions for alkali ions with butanone and cyclohexanone molecules.

Acknowledgment. J. M. Lucas, J. de Andrés, M. Albertí, and A. Aguilar acknowledge financial support from the Spanish Ministerio de Educación y Ciencia (Project CTQ2007-61109). Thanks are also due to the Centre de Supercomputació de Catalunya (CESCA) and to the Fundació Catalana per a la Recerca for allocating supercomputing time. Also J. M. Bofill acknowledges financial support from the Spanish Ministerio de

Educación y Ciencia (Project CTQ2008-02856/BQU) and from Generalitat de Catalunya 2005SGR-00111.

References and Notes

(1) Wieting, R. D.; Staleym, R. H.; Beauchamp, J. L. *J. Am. Chem. Soc.* **1975**, *97*, 924 and references therein.
(2) Allison, J.; Ridge, D. P. *J. Am. Chem. Soc.* **1979**, *101*, 4998.
(3) Hogg, A. M.; Kebarle, P. *J. Chem. Phys.* **1965**, *43*, 449.
(4) Perl, J.; Daley, H. L.; Peek, J. M.; Green, T. A. *Phys. Rev. Lett.* **1969**, *23*, 677.
(5) Aquilanti, V.; Casavecchia, P. *J. Chem. Phys.* **1976**, *64*, 751 and refeences therein.
(6) Olsen, J. Ø.; Andersen, N.; Andersen, T. *J. Phys. B* **1977**, *10*, 1723.
(7) Aquilanti, V. *Z. Phys. Chem.* **1974**, *90*, 1.
(8) McMillan, W. L. *Phys. Rev. A* **1971**, *4*, 69.
(9) Sogas, J.; Aricha, M. E.; de Andrés, J.; Albertí, M.; Lucas, J. M.; Aguilar, A. *Phys. Chem. Chem. Phys.* **2001**, *3*, 3638. and references cited therein.
(10) Sabidó, M.; de Andrés, J.; Sogas, J.; Lucas, J. M.; Albertí, M.; Bofill, J. M.; Aguilar, A. *Phys. Chem. Chem. Phys.* **2005**, *7*, 310 and references therein.
(11) Sabidó, M.; de Andrés, J.; Sogas, J.; Lucas, J. M.; Albertí, M.; Bofill, J. M.; Aguilar, A. *J. Chem. Phys.* **2005**, *123*, 124314.
(12) Sabidó, M.; de Andrés, J.; Sogas, J.; Lucas, J. M.; Albertí, M.; Bofill, J. M.; Rabadán, I.; Aguilar, A. *Eur. Phys. J. D* **2008**, *47*, 63.
(13) Sogas, J.; Sabidó, M.; de Andrés, J.; Lucas, J. M.; Albertí, M.; Aguilar, A. *Chem. Phys. Lett.* **2006**, *425*, 234.
(14) Lambert, D. L. *Phys. Scr. T* **1994**, *47*, 186.
(15) Märk, T. D.; Peterson, K. I.; Castelman, A. W., Jr. *Nature* **1980**, *285*, 392. Schlosser, G.; Takáts, Z.; Vékey, K. *J. Mass Spectrom.* **2003**, *38*, 1245. Seinfeld, J. H.; Pandis, S. N. *Atmospheric Chemistry and Physics: from Air Pollution to Climate Change*; Wiley-Interscience: New York, 1997.
(16) Lippard, S. J.; Berg, J. M. *Principles of Bioinorganic Chemistry*; University Science Books: Mill Valley, CA, 1994.
(17) Hoyau, S.; Norrman, K.; McMahon, T. B.; Ohanessian, G. *J. Am. Chem. Soc.* **1999**, *121*, 8864.
(18) Castleman, A. W.; Holland, P. M.; Lindsay, D. M.; Peterson, K. I. *J. Am. Chem. Soc.* **1978**, *100*, 6039. Castleman, A. W.; Peterson, K. I.; Upschulte, B. L.; Schelling, F. J. *Int. J. Mass Spectrom. Ion Phys.* **1983**, *47*, 203. Guo, B. C.; Conklin, B. J.; Castleman, A. W. *J. Am. Chem. Soc.* **1989**, *111*, 6506. Guo, B. C.; Purnell, J. W.; Castleman, A. W. *Chem. Phys. Lett.* **1990**, *168*, 155.
(19) Rodgers, M. T.; Armentrout, P. B. *J. Phys. Chem. A* **1999**, *103*, 4955.
(20) Armentrout, P. B.; Rodgers, M. T. *J. Phys. Chem. A* **2000**, *104*, 2238.
(21) Aikens, C. M.; Webb, S. P.; Bell, R. L.; Fletcher, G. D.; Schmidt, M. W.; Gordon, M. S. *Theor. Chem. Acc.* **2003**, *110*, 233.
(22) Fujii, T. *Mass Spectrom. Rev.* **2000**, *19*, 111.
(23) *Lithium Chemistry: A theoretical and Experimental Overview*; Sapse, A.-M., Scheleyer, P. v. R., Eds.; Wiley: New York, 1995.
(24) Loupy, A.; Tchoubar, B. *Salt Effects in Organic and Organometallic Chemistry*; VCH: Weinheim, 1992.
(25) Jarek, R. L.; Miles, T. D.; Trester, M. L.; Denson, S. C.; Shin, S. K. *J. Phys. Chem. A* **2000**, *104*, 2230.
(26) McMahon, T. B.; Ohanessian, G. *Chem. Eur. J.* **2000**, *6*, 2931.
(27) Operti, L.; Rabezzana, R. *Mass Spectrom. Rev.* **2003**, *22*, 407.
(28) Ye, S. J.; Clark, A. A.; Armentrout, P. B. *J. Phys. Chem. B* **2008**, *112*, 10291.
(29) Sabidó, M.; Lucas, J. M.; de Andrés, J.; Sogas, J.; Albertí, M.; Aguilar, A.; Bassi, D.; Ascenzi, D.; Franceschi, P.; Tosi, P.; Pirani, F. *Chem. Phys. Lett.* **2007**, *442*, 28.
(30) Woodin, R. L.; Beauchamp, J. L. *Chem. Phys.* **1979**, *41*, 1.
(31) Lucas, J. M.; de Andrés, J.; Sogas, J.; Albertí, M.; Bofill, J. M.; Bassi, D.; Ascenzi, D.; Tosi, P.; Aguilar, A. *J. Chem. Phys.* **2009**, *131*, 024306.
(32) Creasy, W. R.; Farrar, J. M. *J. Chem. Phys.* **1987**, *87*, 5280.
(33) Teloy, E.; Gerlich, D. *Chem. Phys.* **1974**, *4*, 417.
(34) Tosi, P.; Fontana, G.; Longano, S.; Bassi, D. *Int. J. Mass Spectrom. Ion Process* **1989**, *93*, 95.
(35) Gerlich, D. *Adv. Chem. Phys.* **1992**, *82*, 1.
(36) Ervin, K. M.; Armentrout, P. B. *J. Chem. Phys.* **1985**, *83*, 166.
(37) Tosi, P. *Chem. Rev.* **1992**, *92*, 1667.
(38) Pullins, S. T.; Dressler, R. A.; Torrens, R.; Gerlich, D. *Z. Phys. Chem.* **2000**, *214*, 1279.
(39) Chantry, P. J. *J. Chem. Phys.* **1971**, *55*, 2746.
(40) Lifshitz, C.; Wu, R. L. C.; Tiernan, T. O.; Terwillger, D. T. *J. Chem. Phys.* **1978**, *68*, 247.
(41) Schlier, C. G. *Chem. Phys.* **1971**, *55*, 2746.
(42) Levine, R. D.; Bernstein, R. B. *Molecular Reaction Dynamics and Chemical Reactivity*; Oxford University Press: New York, Oxford, 1987.
(43) Schmidt, M. W.; Baldridge, K. K.; Boatz, J. A. *J. Comput. Chem.* **1993**, *14*, 1347. *Computer code GAMESS*, version 20, Iowa State University, 2006.
(44) Dunning, T. H. *J. Chem. Phys.* **1971**, *55*, 761.
(45) McLean, A. D.; Chandler, G. S. *J. Chem. Phys.* **1980**, *72*, 5639.
(46) Gianinetti, E.; Raimondi, M.; Tornaghi, E. *Int. J. Quantum Chem.* **1996**, *60*, 157.
(47) Varandas, A. J. C. *J. Chem. Phys.* **2007**, *127*, 114316.
(48) Schmid, R.; Miah, A. M.; Sapunov, V. N. *Phys. Chem. Chem. Phys.* **2000**, *2*, 97.
(49) Moision, R. M.; Armentrout, P. B. *J. Phys. Chem A* **2002**, *106*, 10350.
(50) Clary, D. C.; Henshaw, J. P. *Faraday Discuss. Chem. Soc.* **1987**, *84*, 333.
(51) Albertí, M.; Prieto, M.; Aguilar, A. *J. Chem. Soc., Faraday Trans.* **1992**, *88*, 1615.
(52) Dunbar, R. C. *Int. J. Mass Spectrom. Ion Process.* **1990**, *100*, 423.
(53) Langevin, M. P. *Ann Chim. Phys.* **1905**, *5*, 245. Gioumousis, G.; Stevenson, D. P. *J. Chem. Phys.* **1958**, *29*, 294. Dugan, V.; Magee, J. L. *J. Chem. Phys.* **1967**, *47*, 3103. Su, T.; Bowers, M. T. *J. Chem. Phys.* **1973**, *58*, 3027. Bass, L.; Su, T.; Chesnavich, W. J.; Bowers, M. T. *Chem. Phys. Lett.* **1975**, *34*, 119 and references therein.
(54) McQuarrie, D. A.; Simon, J. D. *Physical chemistry: a molecular approach*; University Science Books, 1997; Chapter 18.

JP904910D